Constraints of FL Motif on the Targeting and Function of Sodium-Bicarbonate Cotransporter 1

Hong C Li[1], Ali Shawki[2], YoonKyung Park[3], Emily Y Li[1] , Kyung-Soo Hahm[3], Joel H. Collier[4] , Bryan Mackenzie[2] and Manoocher Soleimani[1,5].

[1]Medicine, University of Cincinnati, Cincinnati, OH, United States,

[2] Molecular and Cellular Physiology, University of Cincinnati, Cincinnati, OH, United States,

[3] Research Center for Proteineous Materials, Chosun University, Kwangju, Korea,

[4] Department of Surgery, University of Chicago, IL, United States

[5] Research Services, Veterans Administration Hospital, Cincinnati OH United States

ABSTRACT

A C-terminal dihydrophobic **FL** motif plays a vital role in the basolateral targeting of sodium bicarbonate cotransporter 1. To further characterize the role of dihydrophobic **FL** motif, 1). the **FL** motif in wild type (P**FL**S) was reversed to **LF (**P**LF**S**)**, 2). the **FL** motif (P**FL**S) was shifted upstream (**FL**PS), and 3). the **FL** motif (P**FL**S) was shifted downstream (PS**FL**). The wild type (P**FL**S) and its mutant (P**LF**S) were exclusively expressed on the basolateral membrane by con-focal microscopy, however, the mutant (**FL**PS) and (PS**FL)** were predominantly mistargeted to the apical membrane and the cytoplasm, respectively. Functional studies showed that the mutant (PS**FL**) displayed a remarkably reduced current (p value<0.05 vs wild type). The mutant (PS**FL**) displayed a more reduced membrane surface expression than the wild type and was co-localized with ER marker. The protein sequence spanning **FL** motif in kNBC1 C-terminal cytoplasmic tail shows α helical structure, mutants (P**LF**S) and (PS**FL**) reduce α-helical contents by circular dichroism study. Reversed FL isn't a constraint for basolateral targeting, but shifting it upstream and downstream are ones.

KEYWORDS: Basolateral targeting, mutations with reversed and altered relative position of motif, alpha helical structure.

INTRODUCTION

Polarization of epithelial cells in animals is critical to their physiological functions, and involves the precise sorting, trafficking and targeting of asymmetrical transmembrane proteins to the apical and basolateral membrane domains (Tepass et al., 2001).

Possible mechanisms by which proteins are targeted to the apical membrane include N-linked glycosylation (Scheiffele, et al., 1995;Gut, et al., 1998) and intracellular association with glycosphingolipids(GPI) (Brown and Rose, 1992). GPI-linked proteins destined for the apical membrane are preferentially delivered to plasma-membrane microdomains (lipid rafts) rich in cholesterol, glycolipids and sphingolipids (Simons & Ikonen, 1997; Ikonen, 2001). Influenza virus hemagglutinin and neuraminidase contain apical targeting signals identified both within and outside of transmembrane domains which can bind lipid rafts and specify apical sorting (Kundu et al, 1996; Mackenzie et al., 1999; Lin et al., 1998; Barman et al., 2001; Theodore and Caplan, 2003).

In contrast, few models based on specific N- or C-terminal cytoplasmic motifs exist for basolateral targeting of proteins. For example, tyrosine-containing motifs NPXY/YXXφ(in which φ is a bulky or hydrophobic residue) were identified in the low-density lipoprotein receptor(LDL-R)(Matter et al., 1992), the vesicular stomatitis virus glycoprotein(VSVG)(Thomas, et al., 1993), the polymeric immunoglobulin A receptor(pIgA-R), the tranferrin receptor(Tfr-R)(Mackenzie et al., 2007) and the anion exchanger 1(AE1)(Matter, et al., 1994; Matter & Mellman, 1994; Devonald et al., 2003). All of these tyrosine-containing motifs are believed to direct the basolateral targeting of

these transmembrane proteins and mutation of tyrosine to alanine in these motifs disrupts the exclusively basolateral targeting of these proteins.

Whereas basolateral targeting of the IgG Fc receptor FcRII-B2(FcR) does not depend on two tyrosine residues in its cytosolic domain, a di-leucine motif within a short 13 amino acid domain mediates basolateral delivery of FcR (Hunziker and Fumey, 1994; Matter, et al., 1994). Di-leucine motifs are also believed to be important for the basolateral targeting of E-cadherin, nucleotide pyrophosphatase/phosphodiesterase1 (NPPase1), the sulfate anion transporter sat-1 and the ClC2 chloride channel which are asymmetrically distributed in epithelial cells (Miranda, et al., 2001; Bello, et al., 2001; Regeer and Markovich, 2004; Pena-Munzenmayer, et al., 2005). Such signals are not limited to di-leucine motifs, however, as other leucine containing dihdrophobic targeting motifs include a Leu-Val(LV) motif in the resident plasma-membrane adhesion protein CD44 (Sheikh and Isacke, 1996) and a Leu-Eil(LI) motif in the plasma-membrane Ca^{2+}-ATPases(PMCA1b and PMCA2b)(Grati et al., 2006).

Other di-hydrophobic motifs proposed to direct basolateral targeting begin with valine(V), including the VV motif(residues 333-334) in the carboxyl-terminal cytoplasmic portion of the basolateral Kir4.1 K^+ channel in renal distal tubules(Tanemoto et al., 2005) and the VW motif in the N-terminal cytoplasmic domain of the sodium-dependent dicarboxylate transporter(NaDC3) expressed in MDCK and LLC-PK1 cells(Bai et al., 2006).

A novel motif beginning with F is the di-hydrophobic FL motif, which plays a vital role in the basolateral targeting of the sodium bicarbonate cotransporter(NBC1, SLC4A4) in MDCK cells(Li et al., 2004; Li et al., 2007). Recently, the FL di-hydrophobic motif

was shown to play a vital role in the basolateral targeting of NBC1 in MDCK cells. NBC1 functions in tandem with the apical Na^+/H^+ exchanger 3 (NHE3) in the kidney proximal tubule to ensure the reabsorption of the majority of filtered bicarbonate (Soleimani and Burnham, 2001; Soleimani, 2002; Soleimani, 2003; Romero, et al., 2004; Romero, 2005; Abuladze, et al., 2005; Pushkin and Kurtz , 2006; Boron, 2006). Mutations in NBC1 were associated with bicarbonate wasting and proximal renal tubular acidosis in human patients (Igarashi et al., 1999; Igarashi et al., 2001; Usui, et al., 2001; Alper, 2002; Dinour et al., 2004; Horita, et al., 2005) and resulted in mistargeting to the apical membrane or the cytoplasm in MDCK polarized cells(Li et al., 2005; Toye et al., 2006).

Whereas the list of basolateral signal determinants is constantly increasing, few investigations have involved further characterization and specific constraints of these di-hydrophobic motifs. In order to better understand the role of basolateral di-hydrophobic motifs(LL, LV, LI; VV, VW; FL) in basolateral-membrane targeting, we have manipulated the composition or placement of the di-hydrophobic FL motif of the renal NBC1(kNBC1) in the following manners: (1) We reversed the FL motif to LF in order to test whether its specific orientation is a constraint for targeting, (2) We shifted the FL motif downstream or upstream by one amino-acid residue to test whether the flexibility of the di-hydrophobic FL motif in terms of primary sequence is congruous.

We examined the subcellular targeting and functional activity of epitope-tagged kNBC1 mutants expressed in transiently-transfected MDCK cells and in *Xenopus* oocytes using confocal microscopy and voltage clamping. We also examined circular

dichroism of wild type and mutant kNBC1 di-hydrophobic motif in short peptides synthesized in vitro in order to explore their secondary structures.

RESULTS

Epitope-tagged NBC1 Is Targeted Exclusively to the Basolateral Membrane in MDCK Epithelial Cells. In the first series of experiments, we examined the expression of GFP vector without the NBC1 insert in MDCK cells. **Fig. 1a.** (**x-y projection**) shows that transfection of cultured cells with the GFP vector alone (no NBC1 insert) results in the accumulation of GFP in the cytoplasm and no localization on the membrane(**Fig. 1a.** co-labeled with ZO-1 staining and in **Supplementary Fig. 8a**. phallodin-tetramethylrhodamine staining). However, transfection with the GFP-NBC1 full-length cDNA shows exclusive localization in the membrane (as visualized by **x-y projections, front view**) in cells (**Fig. 1b, top and middle panels,** co-labeled with ZO-1 staining). Z-line image analysis (**bottom panel, x-z projection**) indicates that NBC1 is exclusively detected on the basolateral membrane, which is also confirmed in the polarized MDCK cells co-stained with phallodin-tetramethylrhodamine and PNA-lectin in **Supplementary Fig. 8b**. The results in **Fig. 1b** and Supplementary **Fig. 8b.** are consistent with published reports on the basolateral membrane localization of NBC1 in epithelial cells (Schmitt, et al., 1999; Thevenod, et al., 1999; Roussa, et al., 1999; Bok, et al., 2001; Satoh, et al., 2003; Yamada, et al., 2003; Li, et al., 2004; Li, et al., 2005; Toye, et al., 2006; Li, et al., 2007).

Epitope-tagged NBC1 Mutant 1 with Reversed Di-hydrophobic FL Motif Is Targeted Exclusively to the Basolateral Membrane in MDCK Epithelial Cells. Similarly to the GFP-NBC1 wild type, transfection with the GFP-NBC1 mutant 1 with a reversed di-hydrophobic FL motif shows exclusive localization in the membrane in cells (as visualized by **x-y projections, front view**, **Fig. 2c, top and middle panels,** co-labeled

with ZO-1 staining). Z-line image analysis (**bottom panel, x-z projection**) indicates that NBC1 is exclusively detected on the basolateral membrane, which is also confirmed in the polarized MDCK cells co-stained with phallodin-tetramethylrhodamine in **Supplementary Fig. 8c**.

Epitope-tagged NBC1 Mutant 2 with a Di-hydrophobic FL Motif Shifted Upstream Is Mistargeted to the Apical Membrane in MDCK Epithelial Cells. Unlike GFP-NBC1 wild type and mutant1, GFP-NBC1 mutant 2 with di-hydrophobic FL motif shifted upstream shows apical localization in the membrane in cells(as visualized by **x-z projections, side view**, **Fig. 2d, top panel,** co-labeled with ZO-1 staining). Z-stack images (**bottom and middle panels, x-y projections**) indicate that this NBC1 mutant 2 is detected on the plasma membrane. Apical localization of GFP-NBC1 mutant 2 with the di-hydrophobic FL motif upstream shifted is also confirmed in the polarized MDCK cells co-stained with phallodin-tetramethylrhodamine and PNA-lectin in **Supplementary Fig. 8d**.

Epitope-tagged NBC1 Mutant 3 with Di-hydrophobic FL Motif Shifted Downstream Is Mistargeted to the Cytoplasm in MDCK Epithelial Cells. In contrast to GFP-NBC1 wild type, mutant1 and mutant 2, GFP-NBC1 mutant 3 with a di-hydrophobic FL motif shifted downstream shows dominant cytoplasmic localization in cells (as visualized by **x-y projections, front view**, **Fig. 2e., bottom and middle panels,** co-labeled with ZO-1 staining). Z-line image analysis (**top panel, x-z projection**) indicates that NBC1 mutant 3 is also detected on the apical membrane. This result is also confirmed in the polarized MDCK cells co-stained with phallodin-tetramethylrhodamine and PNA-lectin in **Supplementary Fig. 8e**.

Epitope-tagged NBC1 Mutants Which Are Targeted to the Plasma Membrane Exhibit Comparable Wild Type NBC1 Functional Activities, Whereas the Epitope-tagged NBC1 Mutant Which Is Mistargeted to the Cytoplasm Shows a Significantly Reduced Functional Activity. We expressed wild type and its various mutant cRNAs in *Xenopus* oocytes to examine the effect of the specific orientation and relative positions of the dihydrophobic motif FL on kNBC1 functional activity. We superfused oocytes with standard 96 mM NaCl medium(ND96) or medium in which 33 mM NaCl was replaced by 33 mM HCO_3^- equilibrated with 5% CO_2 at room temperature, and measured bicarbonate-induced currents. The current/voltage relationships of kNBC1 mutant 1 and 2 did not differ from those of the kNBC1 wild type. The kNBC1 mutant 3 also mediated bicarbonate-induced currents, but they were significantly smaller than those of wild type ($p<0.01$, in **Fig. 3.**).

Epitope-tagged NBC1 Mutant 3 with Di-hydrophobic FL Motif Shifted Downstream Is Reduced on Oocyte Surface Membrane and Co-localized with ER Marker PDI in Polarized MDCK Cells. The above experiments indicated that kNBC1 mutants 1 and 2 which did not mistarget to the cytoplasm, show comparable functional activities to, wild type NBC1, whereas kNBC1 mutant 3 which mistargets into the cytoplasm, exhibits a significantly reduced functional activity in frog oocytes. To investigate whether kNBC1 mutant 3 exhibits a similar localization pattern in the frog oocytes where functional activity was carried out, *X. laevis* oocytes were injected with GFP, full-length GFP-kNBC1 and its mutants cRNAs to determine if the expressed proteins are in detergent fractions or non-detergent fractions. The cRNA injected oocytes were homogenized in lysis buffers with or without 1% Trition X-100, and fractioned mixtures were loaded onto SDS-PAGE gel for western blot analysis. Rabbit anti-GFP serum was used to detect the

GFP signal. As shown in **Fig.4.**, the fractionated protein mixtures extracted with or without detergent from the oocytes injected with GFP cRNA showed equivalent strong signals, whereas the fractionated protein mixtures extracted by the detergent from the oocytes injected with GFP-kNBC1 wild type and mutant cRNAs showed stronger signals than those extracted without detergent. Membrane proteins can only be extracted with detergents, so these results for GFP-kNBC1 wild type, mutant 1 and 2 proteins in detergent fractions are consistent with their membrane localization in MDCK cells and functional activities in frog oocytes. Considering the GFP-kNBC1 mutant 3 mistargeting to the cytoplasm in MDCK cells and the reduced functional activity in oocytes, this result may indicate be interpreted that this mutant 3 protein is mainly expressed in the cytoplasm on membranes other than the plasma membrane, such as ER or mitochondria. etc) in the cytoplasm. To explore this possibility, we expressed GFP-kNBC1 wild type and mutant 3 in frog oocytes immunostained with rabbit anti-GFP serum as well as in polarized MDCK cells co-stained with ER marker, PDI antibody. As in **Fig.5.**, GFP-kNBC1 protein expression on plasma surface membrane was more reduced on the oocytes injected with GFP-kNBC1 mutant 3 cRNA than the one injected with GFP-kNBC1 wild type cRNA, while no GFP signal on plasma surface membrane was detected on the oocytes injected with GFP cRNA. In the following experiment, the epitope-tagged kNBC1 mutant 3 plasmid DNA was transiently transfected into polarized MDCK cells again. As shown in **Fig.6.**, the epitope-tagged kNBC1 wild type was not co-localized with PDI(protein disulfide isomerase, red) ER marker in MDCK cells, however, the epitope-tagged kNBC1 mutant 3 was shown to co-localize with PDI in the cytoplasm in the transfected MDCK cells.

*Dihydrophobic **FL** Motif in kNBC1 C-terminal Cytoplasmic Tail Shows α Helical Structure, Reversing and Shifting Downstream **FL** Motif Cause Reduced α Helical Contents.* The purpose of the next series of experiments was to characterize the secondary structure of kNBC1 C-terminal cytoplasmic tail containing dihydrophobic FL motif by circular dichroism. Three short peptides with 20 amino acid residues were designed and synthesized, purified with preparative HPLC chromatography. Peptide 1: kNBC1 wild type I1001-S1020, IKIPMDIMEQQP**FL**SDSKPS; peptide 2: kNBC1 mutant 1 I1001-S1020, IKIPMDIMEQQP**LF**SDSKPS and peptide 3: kNBC1 mutant 3 I1001-S1020, IKIPMDIMEQQPS**FL**DSKPS and their purities are all more than 95%.

CD spectra data sets were collected from 190 nm to 250 nm. Data sets from 209 nm to 250 nm are validated and used to interpret the results. **Fig.7a**. shows CD spectra of kNBC1 wild type, mutant 1 and mutant 3 short peptides in sodium phosphate buffer(pH7.2). Overall, kNBC1 wild type shows more negative differential absorptions than mutant 1 and mutant 3. It was calculated that kNBC1 wild type, mutant 1 and mutant 3 short peptides contain 27.3%, 22.6% and 16.8% α helical contents in 10 mM sodium phosphate buffer(pH7.2), respectively, as shown in **Table 1**. Similarly, **Fig.7b**. shows CD spectra of kNBC1 wild type, mutant 1 and mutant 3 short peptides in 50% TFE buffer. Again, kNBC1 wild type shows more negative differential absorptions than mutant 1 and mutant 3 under α helical structural inducing condition. It was calculated that kNBC1 wild type, mutant 1 and mutant 3 short peptides contain 54.7%, 42.4% and 30.9% α helical contents in 50% TFE buffer, respectively, as shown in **Table 1**. All these data showed that reversing di-hydrophobic motif **FL** (mutant 1) or shifting downstream **FL** motif (mutant 3) may cause a reduced α helical content under conditions of either α helical

structural non-induction or induction.

To summarize the CD experiments, the amino acid residue region near di-hydrophobic FL motif in C-terminal cytoplasmic tail of kNBC1 exhibited a typical α-helical structure(27.3% α-Helix in sodium phosphate buffer vs.54% α-Helix in 50% TFE buffer), whereas kNBC1 mutant 1 with reversed FL motif (specific orientation altered)and mutant 3 with downstream shifted FL motif(relative position altered) showed lesser α-helical contents. Combined with basolateral or cytoplasmic targeting phenotypes of kNBC1 mutant 1 and 3 in polarized MDCK cells, we propose that maintaining a certain amount of α-helical structure contents near di-hydrophobic FL motif in C-terminal cytoplasmic tail of kNBC1 may be one of factors for it to target exclusively to the basolateral membrane in epithelial cells and to function in frog oocytes, as a greatly reduced α-helicity may not be favorable for NBC1 to target on the basolateral membrane and causes a loss of its functional activity to some degrees.

Discussion

The specific orientation and relative positions(flexibility of primary sequence) of di-hydrophobic FL motif in kNBC were tested to be constraints of basolateral targeting and functional activities. Firstly, targeting of NBC1 to the basolateral membrane was examined in the polarized MDCK cells using NBC1 mutants either with FL reversed motif or FL upstream and downstream shifted motifs, generated by site directed mutagenesis. The results demonstrated that the full length NBC1 is targeted to the basolateral membrane, consistent with published reports(**Fig. 1b.** and **Supplementary Fig. 8b.**), with GFP as control being expressed in cytoplasm as well as nuclei of epithelial cells (**Fig.1a.** and **Supplementary Fig. 8a.**). Site-directed mutagenesis in the carboxyl terminal tail of NBC1 with reversed FL motif, GFP-kNBC1 mutant 1, resulted in no distinct trafficking patterns from GFP-kNBC1 wild type phenotype(**Fig. 2a.** and **Supplementary Fig. 8c.**), The membrane trafficking of GFP-kNBC1 mutant 1 in epithelial cell model is supported by its expression and functional activity analysis in frog oocytes. As in **Fig.3.**, there is no significant difference of currents and voltage measurements between GFP-kNBC1 wild type and mutant 1($p>0.05$). Western blots showed that GFP-kNCB1 mutant 1 proteins are detergent fractionated and the results are consistent with its plasma membrane localization in MDCK cells. The GFP-kNBC1 mutant 1 transiently transfected MDCK cells co-stained with ER marker PDI antibody showed no co-localization(data not shown). Based upon all of these data, we make a conclusion that specific orientation of di-hydrophobic motif FL is not a constraint for kNBC1 to target basolateral membrane in polarized MDCK cells, causing no functional activity loss of transporting bicarbonate into frog oocytes. Our previous works showed

that GFP-kNBC1 mutant FF(di-hydrophobic motif FL>FF) targets on basolateral membrane and GFP-kNBC1 LL(di-hydrophobic motif FL>LL) mistargets into cytoplasm in the polarized MDCK cells(Li, et al., 2007). All these data showed that F(phenylalanine) is a "dominant" amino acid residue in comparison with L(leucine) in di-hydrophobic FL motif. The "dominant" amino acid residue F can replace the other amino acid residue L without altering basolateral targeting pattern in transmembrane protein kNBC1, and vice versa it is not true. The precise position of "dominant" amino acid residue F in di-hydrophobic FL motif need not to be fixed(specific orientation of FL motif is not a constraint to target basolaterally) because either FL sequence in wild type or LF sequence in mutant 1 showed similar basolateral targeting pattern and comparable functionality. There is no reason to study this "dominant" amino acid residue effect of di-hydrophobic motif in basolateral transmembrane proteins with LL and VV motifs, because their compositions of di-hydrophobic motif consist of two identical amino acid residues. Neverlessly, our studies arise to the possibility of a similar di-hydrophobic motif constitute signal mechanism also exiting in the basolateral transmembrane proteins with LI, LV and VW motifs. It is also explorable for di-hydrophobic FL motif in basolateral membrane protein kNBC1 to be replaced with the other di-hydrophobic motifs such as VV, VW, LV, LI, or even the tyrosine-based motif NPXY/YXXφ, assuming that they may or may not share the same basolaterally targeting partner proteins, such as subunits of adaptor-protein complexes (Bonifacino et al., 1999; Devonald et al., 2003).

The relative positions(flexibility of primary sequence) of di-hydrophobic FL motif in kNBC were demonstrated to be constraints of basolateral targeting as well as

functionality. At first, a shifting FL motif one amino acid residue upstream(shifting to N-terminus of kNBC1 protein molecule, GFP-kNBC1 mutant 2) caused sodium bicarbonate cotransporter retargeting to the apical membrane (**Fig. 2b.** and **Supplementary Fig. 8d.**). Like the other apically mistargeting GFP-kNBC1 mutants{FL>AL:(F1013A) and FL>FA(L1014A)}exhibiting comparable hyperpolarized membrane potentials in oocytes exposed to bicarbonate(Li, et al., 2004), GFP-kNBC1 mutant 2 with FL upstream shifted in oocytes showed no significant difference of currents and voltage measurements from GFP-kNBC1 wild type($p>0.05$), as in **Fig.3**. Western blots showed that GFP-kNCB1 mutant 2 proteins are also detergent fractionated. The GFP-kNBC1 mutant 2 transiently transfected MDCK cells co-stained with ER marker PDI antibody showed predominantly plasma membrane localization, with residual co-localized with PDI staining(data not shown).

Secondly, a shifting FL motif one amino acid residue downstream(shifting to C-terminus of kNBC1 protein molecule, GFP-kNBC1 mutant 3) caused significant accumulation of NBC1 in the cytoplasm in the polarized MDCK cells(**Fig. 2c.** and **Supplementary Fig. 8e.**)., along with significantly reduced functional activity($p<0.05$), as in **Fig.3**. Although western blots showed that GFP-kNCB1 mutant 3 proteins are detergent fractionated, its surface expression intensity on oocytes plasma membrane is noticeably reduced in comparison with the GFP-kNBC1 wild type, with GFP control showing background immunostaining signals, as in **Fig.5**. GFP-kNBC1 mutant 3 transiently transfected MDCK cells co-stained with ER marker PDI antibody showed predominantly co-localized with PDI staining(**Fig.6.**). These results showed that a

shifting FL motif one amino acid residue downstream in kNBC1 severely interferes its membrane localization in the epithelial cells.

Although a shifting FL motif to upstream causes no loss of functional activity in frog oocytes system, it may severely interfere the vectorial transport of bicarbonate *in vivo* due to the mistargeting of NBC1 to the apical membrane, causing proximal tubular acidosis due to co-transporting sodium and bicarbonate into the lumen again and less bicarbonate transport back to blood vessel for reabsorption. From the data and discussions mentioned above, we know that the relative position of di-hydrophobic FL motif in kNBC1 protein is very rigid. The non-flexibility of relative position of di-hydrophobic FL motif may conformationally be sustained by the whole kNBC1 protein structure or local short peptide scafford component(s). The expression of an appropriate apically targeting transmembrane protein tagged with various FL motif containing peptides from kNBC1 C-terminal cytoplasmic tail in epithelial cells will help to determine existence of such a component(s), assuming that such FL motif containing amino acid sequence facilitates this apical transmembrane protein to re-target basolaterally in epithelial cells.

Although there are many reports on the mechanisms of basolateral targeting, most of studies focused upon identification of primary amino acid residues responsible for such signals or some related adaptor-protein complexes, few investigations were documented to characterize tertiary or secondary structural analysis of such basolateral targeting motifs. In the present study, we not only investigate the effects of specific orientation and relative position of di-hydrophobic FL motif from kNBC1 on its basolateral targeting and functional activity, but also explore secondary structures of di-hydrophobic FL motif containing short peptide as well as mutant peptides by circular

dichroism spectroscopy. Our study showed that di-hydrophobic FL motif containing short peptide exhibits a typical α helical structure, reversing FL motif or shifting it to C-terminal end causes reduced α helical contents either in the absence or in the presence of α helical structure inducing reagent(**Fig.7.**). Reversing FL motif in kNBC1 with slightly reduced(20%) α helical contents targets to basolaterl membrane and shifting FL motif to C-terminal end in kNBC1 with greatly reduced (40% to 50%)α helical contents mistargets into cytoplasm. Maintaining a certain amount of α-helical structure contents near di-hydrophobic FL motif in C-terminal cytoplasmic tail of kNBC1 may play a role for it to target exclusively to the basolateral membrane in epithelial cells. Further investigations on kNBC1 tertiary structure by more elegant studies such as x-rays diffraction or 2-D NMR would help to further elucidate this issue.

Summarized in Table 2, we conclude, 1): a specific linear orientation of dihydrophobic **FL** motif in kNBC1 C-terminal end is not necessary for its exclusive targeting to the basolateral targeting and function of NBC1; 2): the specificity of relative position of dihydrophobic **FL** motif in kNBC1 is required for its exclusively basolateral targeting; 3): the protein sequence spanning **FL** motif in kNBC1 C-terminal cytoplasmic tail shows α helical structure, reversing or C-terminal shifting of di-hydrophobic FL motif reduces α helical contents in kNBC1.

Materials and methods

Construction of tagged full length NBC1 and mutants. The full-length NBC1 was generated by PCR, using the human full-length kidney NBC1 DNA (3,257 bp and 1,035 amino acid residues) as a template (GenBank #: AF007216). The amplified wild-type NBC1 DNA was fused translationally in-frame to GFP by cloning into pcDNA3.1/NT-GFP-TOPO vector (Invitrogen, Carlsbad, CA).

Site directed mutagenesis was performed using QuikChange Site-Directed Mutagenesis Kit (Stratagene, La Jolla, CA). The schemes in **Diagram. 1** and **Diagram 2** depict the procedures of various mutations generated and primers used. The GFP-kNBC1 mutant 1 with FL reversed motif was generated using its sense and antisense primers and a previously studied GFP-kNBC1 mutant FF cDNA as a template(Li, et al., 2007). In order to generate GFP-kNBC1 mutant 2 with FL motif upstream shifted, the GFP-kNBC1 mutant intermediate 1{ L(1012)L1013)P(1014)S(1015)} was firstly generated using its sense and antisense primers and GFP-kNBC1 mutant LL cDNA as a template, shown in **Diagram 1** . Then, GFP-kNBC1 mutant 2 with FL motif upstream shifted was generated using its sense and antisense primers and GFP-kNBC1 mutant intermediate 1 cDNA as a template. In order to generate GFP-kNBC1 mutant 3 with FL motif downstream shifted, the GFP-kNBC1 mutant intermediate 2{P(1012)F1013)F(1014)L(1015)} was generated using its sense and antisense primers and another previously studied GFP-kNBC1 mutant FF cDNA as a template (Li, et al., 2007). Then, GFP-kNBC1 mutant 3 with FL motif downstream shifted was generated using its sense and antisense primers and GFP-kNBC1 mutant intermediate 2 cDNA as a template, as shown in **Diagram 1**.

Cycling parameters for the QuikChange site-directed mutagenesis experiments were as follows: *segment 1*, 95°C, 30 s, 1 cycle; and *segment 2*, 95°C, 30 s, 55°C, 1 min, 68°C, 10 min, 16 cycles. The sequences of all mutants were confirmed by sequencing at DNA Core Facility, Cornell University.

Transient Expression of Epitope-tagged Wild-Type NBC1 and NBC1 mutants in MDCK Cells. The plasmid pcDNA3.1/NT-GFP-NBC1-TOPO or GFP-NBC1 various mutant constructs were transformed into TOP 10 competent cells and single colonies were picked up for growing in 1ml TB bacterial culture medium and transfer to 50 ml TB culture medium for growing overnight. Qiagen EndoFree Plasmid Maxi Kit (Qiagen, Valencia, CA) was used to prepare and purify endotoxin free plasmids. The MDCK cells were maintained in culture medium (DMEM) supplemented with 25 mM $NaHCO_3$, 10% fetal calf serum, penicillin(50 units/ml) and streptomycin (50μg/ml) and incubated at 37°C, 5% CO_2/95% air. MDCK cells were transiently transfected with the epitope-tagged NBC1 full-length and its mutants and studied 48-72 hours later according to established methods (Li, et al., 2004; Li, et al., 2005; Li, et al., 2007). Briefly, cells were seeded on coverslips and transfected at 80%-90% confluence using 1 μg of DNA and 4 μl of Lipofectamine 2000 (Invitrogen, Carlsbad, CA). The transfection efficiency was monitored using PCMV-SPORT β-gal plasmid as control. Changes in cell color in response to X-gal addition was used as marker for beta-gal expression. All cells were co-labeled with ZO-1 antibody staining, or Phalloidin-Tetramethylrhodamine and PNA-lectin Alexa Fluor 568 conjugate, as markers of membrane labeling. The transient expression experiments were conducted three times independently for each construct. The images co-labeled with phalloidin were used as preliminary dada analysis or

recorded for the manuscript publication purposes.

Confocal Microscopy and Immunofluorescence Labeling of Epitope-tagged NBC1 and its Various Mutants. The polarized MDCK cells were washed with PBS, and fixed in 4% formaldehyde/PBS solution as described (Li, et al., 2004; Li, et al., 2005, Li, et al., 2007). For co-labeling studies, MDCK cells were co-stained with PNA-lectin Alexa Fluor 568 conjugate (Molecular Probes, Eurogene, OR) for 20-30 minutes. In separate studies cells were permeabilized with 0.1% TX-100 in PBS, washed with PBS and co-stained with Phalloidin-Tetramethylrhodamine(Sigma, St. Louis, MO) for 20-30 minutes. Afterward cells were washed with PBS, and mounted on glass slides in VECTASHIELD mounting medium for fluorescence (Vector Laboratories, Inc., Burlingame, CA). Images were taken on a Zeiss LSM510 confocal microscope. Both Z-line(y-z or x-z projection) and Z-stack(x-y projections) images were obtained using the LSM 5 Image software(Li, et al., 2004; Li, et al., 2005; Li, et al., 2007). Generally, 0.4-1.0 μ m fixed interval cuts were obtained, and 20-30 images were generated as a gallery. Z-stack images were chosen from the first 3 - 6 basal sections, and images (x-y projections) and corresponding z-lines (x-z or y-z projections) were obtained.

Mouse anti ZO-1 antibody purchased from Zymed(catalogue#33-9100, San Francisco, CA) and mouse anti-PDI(protein-disulfide isomerase) purchased from Stressgen Bioreagents(catalogue#SPA-891, Victoria, BC, Canada) were diluted 200 times and used in immunofluorescence labeling of GFP-kNBC1 in MDCK epithelial cells, respectively. Rabbit anti GFP serum purchased from Invitrogen(catalogue#A6455, Carlsbad, CA) was diluted 200 times and used in immunofluorescence labeling of GFP-kNBC1 in frog oocytes. Donkey anti-mouse or rabbit Alexa-Fluor^{R} 568 - conjugated

secondary antibodies were used either in MDCK cells or frog oocytes sections(7 μm) staining according to established methods and as reported from our laboratory (Petrovic, et al., 2003; Li, et al., 2007). Three slides from every independent transient expression experiments were stained, three independent transient transfections were carried on each construct. More than one clone for each construct were generated when it was necessary to rule out the false negative.

We transiently transfected GFP-kNBC1 wild type and mutants cDNAs extensively in coverlips-grown polarized MDCK cells in term of preliminary data as well as publication quality images. For any new and important discoveries, we also expressed the related plasmid constructs in filter-grown polarized MDCK cells to further confirm what we observed previously. A 24 wells cluster with 0.4 μm pore size filters(Costar) was used to grow MDCK cells and the filter-grown polarized MDCK cells were transiently transfected with endotoxin free plasmid DNAs of GFP, GFP-kNBC1 wild type and mutant 1, 2 & 3, followed by sample preparations and confocal microscopy observations.

Functional Expression of NBC1 Full-Length and Its Various Mutants in Oocytes. Stage IV-V oocytes were isolated as previously described and used for expression studies according to established methods(Xu, et al., 2003; Li, et al., 2004; Li, et al., 2005; Li, et al., 2007). The capped tagged NBC1 (GFP-NBC1 full-length, GFP-NBC1 point-mutations and GFP only) cRNAs were generated using mMESSAGE mMACHINE^{TM} T7 Kit (Ambion, Inc., Austin, TX) according to manufacturers instruction. Fifty nanoliters cRNA (0.5 μg/μl) was injected with a Drummond 510 microdispenser via a sterile glass pipette with a tip of 20-30 μm. After injection, the oocytes were maintained in a solution of the following composition (in mM): 96 NaCl, 2.0 KCl, 1.0 $MgCl_2$, 1.8 $CaCl_2$, 5 Hepes,

2.5 Na pyruvate, 0.5 theophylline, 100U/ml penicillin and 100 µg/ml streptomycin; pH 7.5. Injected oocytes were stored in an incubator at 17^0C and were used for electrophysiological experiments after two to four days.

For voltage and currents measurements, epitope-tagged kNBC1 constructs were used. Briefly, Oocytes were placed on a nylon mesh in a perfusion chamber and continuously perfused(3 ml/min perfusion rate). The perfusion solution had the following composition (in mM): 96 NaCl, 2 KCl, 1 $MgCl_2$, 1.8 $CaCl_2$ and 15 Hepes; pH 7.5. After a stabilization period, the perfusion solution was switched to a CO_2/bicarbonate-containing solution of the following composition (in mM): 30 $NaHCO_3$, 33 TMACl, 66 NaCl, 2 KCl, 1 $MgCl_2$, 1.8 $CaCl_2$ and 15 Hepes; pH 7.5 and gassed with 5% CO_2. Experiments were performed at room temperature (22-25°C). The NBC1 currents induced in the presence of bicarbonate were measured with various voltages and the data were documented as mean ± SEM.

Western Blot Analysis. To examine the detergent and non-detergent fractions of GFP-kNBC1 and its mutants in frog oocytes, oocytes were homogenized in lysis buffer in the presence or absence of 1% Triton X-100. The homogenized mixture without Triton X-100 was centrifuged at 14,000 g and the resultant supernatant was saved. This fraction is designated as Non-TX100 and is predominantly comprised of the cytosol contents(no any plasma or ER membrane components). The homogenized mixture with 1% Triton X-100 was centrifuged and designated as TX100, which is comprised of both membrane and non-membrane proteins. The lysis buffer without detergent consists of 30 mM Tris, 20 mM MES, 100 mM NaCl, final pH 7.0. When used, one complete protease inhibitor tablet per 10 ml lysis buffer was added(Complete Mini, EDTA-free Protease inhibitor

cocktail tablets, Ref# 11-836-170-001, Roche Diagnostics, Indianapolis, IN, U.S.A.). The lysis buffer with detergent was the same as above, with 1% Triton X-100 added to the mixture(Zou, et al., 2004).Western blot analysis of detergent and non-detergent fractions were performed according to established methods (Li, et al., 2005) using GFP-specific polyclonal antibody (Invitrogen) at 1:500 dilution. Donkey anti-rabbit IgG-horseradish peroxidase (HRP) was used as the secondary antibody (Pierce, Rockford, IL). For estimation of protein loading in Western blots, goat β-actin polyclonal antibody (1:1,000) was used (Santa Cruz Biotechnology, Santa Cruz, CA) as control, with rabbit anti-goat IgG-HRP (1:1,000) as the secondary antibody (The Jackson Laboratory, Bar Harbor, ME). The antigen-antibody complex was detected by chemiluminescence method using SuperSignal West Pico Chemiluminescent Substrate kit (Pierce). The experiments were repeated multiple times and GFP protein expression was normalized by β-actin labeling on the same blot.

Peptide Synthesis. Three peptides, kNBC1 wild type I1001-S1020 [also called as P**FL**S] of the sequence IKIPMDIMEQQP**FL**SDSKPS, kNBC1 mutant 1 I1001-S1020 [also called as P**LF**S] of the sequence IKIPMDIMEQQP**LF**SDSKPS and kNBC1 mutant 3 I1001-S1020[also called as P**SFL**] of the sequence IKIPMDIMEQQP**SFL**DSKPS, were synthesized through solid-state phase synthesis at GenScript Corporation, Piscataway, New Jersey. Peptides were synthesized from C-terminus to N-terminus by Fmoc {N-(9-fluorenyl)methooxycarbonyl}chemistry on an Applied Biosystem 433A peptide synthesizer. The short peptides were started from Fmoc-Ser{tBu(t-butyl)}-Wang Resin(4-Benzyloxybenzyl alcohol resin) and then coupled with next Fmoc protected amino acid in one synthesis cycle with the aid of HOBt(N-

Hydroxybenzotriazole)/DIC(N,N-diisopropylcarbodiimide). After full sequences were completed, they were cleaved from resin by TFA(Trifluoroacetic acid) cocktail solution and crystallized in ether. The crude samples were purified by RP-HPLC C18(Reversed Preparative High Performance Liquid Chromatography) columns under the gradient of ACN(Acrylonitrile)+0.1% TFA and H_2O+0.1 TFA washing buffer and verified by mass spectrometry analysis. All resultant peptides have more than 95% purities.

Circular Dichroism Analysis. CD spectra were recorded at 25 °C on a Jasco 810 spectropolarimeter (Jasco, MD, USA) equipped with a temperature control unit. A 0.1-cm path-length quartz cell was used for a 12.5 mM protein solution. At least five scans were averaged for each sample and the averaged blank spectra were subtracted. Each spectrum was obtained by averaging five scans in the 250-190 nm wavelength range. All CD spectra are reported in mean residue ellipticity, $[\theta]_{MRW}$, in $deg \cdot cm^2 dmol^{-1}$. The α-helical content was determined from the mean residue ellipticities at 222 nm, as indicated in Equation (Maeng, et al., 2001).

$$\% \text{ Helix} = ([\theta]_{obs} \times 100)/\{[\theta]_{helix} \times (1 - 2.57/l)\}$$

where $[\theta]_{obs}$ is the mean-residue ellipticity observed experimentally at 222 nm, $[\theta]_{helix}$ is the ellipticity of a peptide of infinite length with 100% helix population, taken as –39,500 $deg \cdot cm^2 dmol^{-1}$, and l is the peptide length or, more precisely, the number of peptide bonds.

Statistics. Results are given as SEM. Student's t test as well as ANOVA were performed among and between the groups. The data were considered significant if $p < 0.05$.

Materials. Expand Long Template PCR System was purchased from Roche. GFP Fusion TOPO TA Expression Kit and Lipofectamine^{TM} 2000 were purchased from Invitrogen (Carlsbad, CA). mMESSAGE mMACHINE^{TM} T7 Kit was purchased from Ambion, Inc. (Austin, TX). EndoFree Plasmid Maxi Kit was purchased from Qiagen (Valencia, CA). DMEM medium was purchased from Life Technologies. All other chemicals were purchased from Sigma Co. (St. Louis, MO).

Acknowledgement

These studies were supported by National Institute of Health Grants DK 62809 (MS), a Merit Review Award, a Cystic Fibrosis Foundation grant and grants from Dialysis Clinic Incorporated (to M.S).

Figure legends

Fig. 1. Transfection of MDCK cells with GFP vector only (no NBC1 insert) or epitope-tagged wild type NBC1.

1a. Expression of GFP vector only (no NBC1 insert). Z-stack analysis(x-y projection, front view). Green: GFP; red: ZO-1 staining with Alexa-Fluor^{R} 568.

1b. Expression of epitope-tagged wild type NBC1 (1010 QQPFLS 1015). **Top and middle panels. Z-stack(x-y projections, front view) image analysis.** Green: GFP-NBC1; red: ZO-1 staining with Alexa-Fluor^{R} 568. **Bottom panel. Z-line (x-z projection, side view) image analysis.** Green: GFP-NBC1; red: ZO-1 staining with Alexa-Fluor^{R} 568.

Fig. 2. Transfection of MDCK cells with epitope-tagged NBC1 mutants.

2a. Expression of epitope-tagged NBC1 mutant 1 (1010 QQPLFS 1015).Top and middle panels. Z-stack(x-y projections, front view) image analysis. Green: GFP-NBC1; red: ZO-1 staining with Alexa-Fluor^{R} 568.**Bottom panel. Z-line(x-z projection, side view) image analysis.** Green: GFP-NBC1; red: ZO-1 staining with Alexa-Fluor^{R} 568.

2b. Expression of the epitope-tagged NBC1 mutant 2 (1010 QQFLPS 1015). Bottom and middle panels. Z-stack(x-y projections, front view) image analysis. Green: GFP-NBC1; red: ZO-1 staining with Alexa-Fluor^{R} 568.

Top panel. Z-line (x-z projection, side view) image analysis. Green: GFP-NBC1; red: ZO-1 staining with Alexa-Fluor^{R} 568.

2c. Expression of the epitope-tagged NBC1 mutant 3 (1010 QQPSFL 1015). Bottom and middle panels. Z-stack(x-y projections, front view) image analysis.

Green: GFP-NBC1; red: ZO-1 staining with Alexa-Fluor^R 568. **Top panel. Z-line (x-z projection, side view) image analysis.** Green: GFP-NBC1; red: ZO-1 staining with Alexa-Fluor^R 568.

Fig. 3. Currents and voltage relationship of kNBC1 wild type and its mutants Currents and voltage relationship were measured by conventional intracellular microelectrodes in *Xenopus* oocytes 2-4 days after injection with epitope tagged wild type NBC1 or various mutants cRNAs. After an equilibrating period, the perfusion solution was switched to a solution containing 33 mM HCO_3^- and gassed with 5% CO2, 95%O2 at pH 7.5. Step pulses between Vm=-160 and +40 mV were applied. All cRNAs injected are 0.5 μg/μl.

Fig. 4. Western blot analysis of the epitope-tagged kNBC1 and its mutants in frog oocytes. After determination of currents and voltage relationship in *X. laevis* oocytes injected with numerous cRNAs, the oocytes were homogenized in the lysis buffers with or without 1% Trition X-100. The rabbit anti-GFP serum was used to detect the GFP signal either from GFP only or GFP fused kNBC1 proteins. The same blot membranes were normalized with β-actin expression.

Fig. 5. Confocal images of sections of frog oocytes expressing epitope-tagged kNBC1 and mutant 3. Frog *Xenopus laevis* oocytes were injected with GFP, GFP-kNBC1 and GFP-kNBC1 mutant 3 cRNAs. Four days after injection of cRNAs, oocytes were embedded with OCT(Optimal Cutting Temperature) media and frozen on dry ice. Sections were cut 7 μm thick and stained with rabbit anti-GFP serum(1:500) and Alexa-Fluor 568-conjugated secondary antibody(1:200). Scale bar, 50 μm.

Fig.6. Immunostaining of MDCK cells expressing epitope-tagged kNBC1 wild type and mutant 3 with an ER marker antibody, PDI. The polarized MDCK cells were transiently transfected with epitope-tagged kNBC1 wild type and mutant 3 endotoxin free plasmids and co-stained with a mouse anti-PDI antibody(1:500) and Alexa-Fluor 568-conjugated secondary antibody(1:200).

Fig.7. Circular dichroism comparison analysis of kNBC1 wild type and mutant short peptides

7a. CD spectra of kNBC1 wild type, mutant 1 and 3 short peptides in sodium phosphate buffer.

7b. CD spectra of kNBC1 wild type, mutant 1 and 3 short peptides in 50% TFE buffer.

Table 1. Analysis of CD spectra for secondary structure content of peptides.

Table 2. A Summary of structures and functions of kNBC1 and mutants.

Supplementary Figures.

Diagram 1. The procedures of various GFP-kNBC1 mutants generated.

Diagram 2. Primer sequences for NBC1 mutants.

Fig.8. Expression of GFP-kNBC1 and GFP-kNBC1 mutants in MDCK cells co-stained with phallodin or PNA-lectin dyes. A: Expression of GFP vector only(no NBC1 insert). Green, GFP signal; red, phalloidin-tetramethylrhodamine. The green and red colors are denoted as the same in the following descriptions unless indicated specifically. **B: Expression of epitope-tagged wild type NBC1**. **Top panel**: x-y projection; **middle panel:** z-x projection; **bottom panel:** cut(red: PNA-lectin staining). **C: Expression of epitope-tagged NBC1 mutant 1**. **Top panel:** x-y projection; **bottom**

panel: z-x projection; **D: Expression of epitope-tagged NBC1 mutant 2**. **Top panel:** cut(red: PNA-lectin staining); **middle panel:** z-x projection; **bottom panel:** x-y projection; **E: Expression of epitope-tagged NBC1 mutant 3**. **Top panel:** cut(red: PNA-lectin staining); **middle panel:** z-x projection; **bottom panel:** x-y projection.

References

1. Abuladze et al., 2005 N. Abuladze, R. Azimov, D. Newman, P. Sassani, W. Liu, S. Tatishchev, A. Pushkin, and I. Kurtz, Critical amino acid residues involved in the electrogenic sodium-bicarbonate cotransporter kNBC1-mediated transport. *J Physiol.* **565**(2005), pp. 717-730.
2. Alper, 2002 S. L. Alper, Genetic diseases of acid-base transporters. *Annu Rev Physiol* **64**(2002), pp.: 899–923.
3. Bai et al., 2006 X. Bai, X. Chen, Z. Feng, K. Hou, P. Zhang, B.Fu and S.Shi, (2006) Identification of basolateral membrane targeting signal of human sodium-dependent dicarboxylate trasnporter 3. *J. Cell Physiol.* **206**(2006), pp. 821-830.
4. Bello et al., 2001 V. Bello, J.W.Goding, V.Greengrass, A. Sali, V. Dubljevic, C. Lenoir, G.Trugnan and M Maurice, (2001) Characterization of a di-leucine-based signal in the cytoplasmic tail of the nucleotide-pyrophosphatase NPP1 that mediates basolateral targeting but not enocytosis. *Mol.Biol.Cell.* **12**(2001), pp3004-3005.
5. Bok et al., 2001 D.Bok, M.J. Schibler, A. Pushkin, P. Sassani, N. Abuladze, Z. Naser, and and I. Kurtz, Immunolocalization of electrogenic sodium-bicarbonate cotransporters pNBC1 and kNBC1 in the rat eye. *Am J Physiol Renal Physiol* **281**(2001), F920-F935.
6. Boifacino et al., 1999 J. S. Bonifacino and E. C. Dell'Angelica, (1999) Molecular bases for the recognition of tyrosin-based sorting signals. *J Cell Biol*. **145**(1999), pp.923-926.
7. Boron, 2006 W.F. Boron, Acid-base transport by the renal proximal tubule. *J. Am. Soc. Nephrol.* **17**(2006), pp.2368-82.
8. Brown et al., 1992. D.A.Brown and J.K. Rose, Sorting GPI-anchored proteins to glycolipid-enriched membrane subdomains during transport to the apical cell surface. *Cell*. **68**(1992): pp. 533-544.
9. Devonald et al., 2003 M. A. Devonald, A. N. Smith, J. P. Poon, G. Ihrke, and F. E. Karet, (2003) Non-polarized targeting of AE1 causes autosomal dominant distal renal tubular acidosis *Nat. Genet.* **33,** 125-127.
10. Dinour et al., 2004 D. Dinour, M. H. Chang, J.Satoh, B. L. Smith, N. Angle, A. Knecht, I. Serban, E. J. Holtzman and M. F. Romero, A novel missense mutation in the sodium bicarbonate cotransporter (NBCe1/SLC4A4) causes proximal tubular acidosis and glaucoma through ion transport defects. *J Biol Chem.* **279**(2004), pp. 52238-52246.
11. Grati et al., 2006 M.Grati, N.Aggarwal, E.E.Strehler, and R. J. Wenthold, Molecular determinants for differential membrane trafficking of PMCA1 and PMCA2 in mammalian hair cells. *J. Cell Sci.* **119**(2006), pp.2995-3007.
12. Gut et al., 1998 A. Gut, F.Kappeler, N. Hyka, M.S. Balda, H.P. Hauri, and K. Matter, Carbohydrate-mediated Golgi to cell surface tranport and apical targeting of membrane proteins. *EMBO J*.**17**(1998), pp. 1919-1929
13. Horita et al., 2005 S. Horita, H. Yamada, J. Inatomi, N. Moriyama, T. Sekine, T. Igarashi, Y. Endo, M. Dasouki, M. Ekim, L. Al-Gazali, M. Shimadzu, G. Seki, and F. Fujita, Functional analysis of NBC1 mutants associated with proximal

renal tubular acidosis and ocular abnormalities. *J Am Soc Nephrol.* **16**(2005), pp. 2270-2278.

14. Hunziker et al., 1994 W.Hunziker and C. Fumey, A di-leucine motif mediates endocytosis and basolateral sorting of macrophage IgG Fc receptors in MDCK cells. *EMBO J*. **13**(1994), pp.2963-2969.
15. Igarashi et al., 1999 T. Igarashi, J. Inatomi, T. Sekine, S. H. Cha, Y. Kanai, M. Kunimi, K. Tsukamoto, H. Satoh, M. Shimadzu, F. Tozawa, T. Mori, M. Shiobara , G. Seki and H. Endou, Mutations in SLC4A4 cause permanent isolated proximal renal tubular acidosis with ocular abnormalities. *Nat Genet* **23**(1999), pp. 264–266.
16. Igarashi et al., 2001 T. Igarashi, J. Inatomi, T. Sekine, M. Shimadzu, F. Tozawa, Y. Takeshima, T. Takumi, T. Takahashi, N. Yoshikawa, H. Nakamura and H. Endou, S. H. Cha, Y. Kanai, M. Kunimi, K. Tsukamoto, H. Satoh, M. Shimadzu, F. Tozawa, T. Mori, M. Shiobara , G. Seki and H. Endou, Novel nonsense mutation in the Na^+/HCO_3^- cotransporter gene (SLC4A4) in a patient with permanent isolated proximal renal tubular acidosis and bilateral glaucoma. *J Am Soc Nephrol* **12**(2001), pp.713–718.
17. Ikonen , 2001. E. Ikonen, Roles of lipid rafts in membrane transport. *Curr Opin Cell Biol.* **13**(2001), pp.470-477.
18. Kundu et al., 1996 A. Kundu, R.T. Avalos, C.M. Sanderson, and D.:P. Nayak, Transmembrane domain of influenza virus neuraminidase, a type II protein, possesses an apical sorting signal in polarized MDCK cells. *J Virol*.**70**(1996), pp.6508-6515.
19. Li et al., 2004 H. C. Li, R. T. Worrell, J. B. Matthews, H. Husseinzadeh, L. Neumeier, S. Petrovic, L. Conforti, and M. Soleimani**,** Identification of a carboxyl-terminal motif essential for the targeting of Na+-HCO-3 cotransporter NBC1 to the basolateral membrane. *J. Biol. Chem.* **279**(2004), pp. 43190-43197.
20. Li et al., 2005 H. C. Li, P. Szigligeti, R. T. Worrell, J. B. Matthews, L. Conforti, and M. Soleimani, Missense mutations in Na+:HCO3- cotransporter NBC1 show abnormal trafficking in polarized kidney cells: a basis of proximal renal tubular acidosis.*Am J Physiol Renal Physiol.* **289**(2005), pp. F61-71.
21. Li et al., 2007 H.C. Li, E.Y. Li, L. Neumeier, L.Conforti, and M. Soleimani, Identifcation of a novel signal in the cytoplasmic tail of the Na^+:HCO_3^- cotransporter NBC1 that mediates basolateral targeting. *Am J. Physiol.Renal Physiol.* **292**(2007),.pp.F1245-55.
22. Lin et al., 1998 S. Lin, H. Y. Naim, A.C. Rodriquez, and M.G. Roth, Mutations in the middle of the transmembrane domain reverse the polarity of transport of the influenza virus hemagglutinin in MDCK epithelial cells. *J Cell Biol.* **142**(1998), pp51-57.
23. Mackenzie, 1999 B.Mackenzie, Selected techniques in membrane transport. In: *Biomembrane Transport*, Lon J Van Winkle(ed), ch 11, pp327-342, Academic Press, San Diego.
24. Mackenzie et al., 2007 B. Mackenzie, H.Takanaga, N. Hubert, A. Rolfs and M.A. Hediger, Functional properties of multiple isoforms of human divalent metal-ion transporter 1(DMT1). *Biochem J*. **403**(2007), pp59-69.

25. Maeng et al., 2001 C.Y. Maeng, M.S. Oh, I.H. Park, and H.J. Hong, Purification and structural analysis of the hepatitis B virus preS1 expressed from Escherichia coli. *Biochem. Biophys.Res.Commun*. **282**(2001), pp.787-92
26. Matter et al., 1992 K.Matter, W. Hunziker, and I. Mellman, Basolateral sorting of LDL receptor in MDCK cells: the cytoplasmic domain contains two tyrosine-dependent targeting determinants. *Cell*. **71**(1992), pp.741-753.
27. Matter et al., 1994 K.Matter, E.M. Yamamoto, and I.Mellman, Structural requirements and sequence motifs for polarized sorting and endocytosis of LDL and Fc receptors in MDCK cells. *J Cell Biol*. **126**(1994), pp991-1004
28. Matter et al., 1994 K.Matter and I. Mellman, Mechanisms of cell polarity: sorting and transport in epithelial cells. *Curr. Opin. Cell Biol*. **6**(1994), pp. 545-554.
29. Miranda et al., 2001 K. C. Miranda, T. Khromykh, P. Christy, T. L. Le, C. J. Gottardi, A. S. Yap, J.L. Stow, and R. D. Teasdale, A dileucine motif targets E-cadherin to the basolateral cell surface in Kadin-Darby canine kidney and LLC-PK1 epithelial cells. *J. Biol.Chem.***276**(2001), pp22565-22572.
30. Pena-Munzenmayer et al., 2005 G. Pena-Munzenmayer, M. Catalan, I. Cornejo, C.D. Figueroa, J. E. Melvin, M. I. Niemeyer, L. P. Cid, and F. V. Sepulveda, Basolateral localization of native ClC-2 chloride channels in absorptive intestinal epithelial cells and basolateral sorting encoded by a CBS-2 domain di-leucine motif. *Journal of Cell Science*, **118**(2005), pp. 4243-4252.
31. Pushkin et al., 2006 A. Pushkin and I. Kurtz, SLC4 base(HCO_3^-, CO_3^{2-}) transporters: classification, function, structure, genetic diseases, and knockout models. *Am J Physiol Renal Physiol*. **290**(2006), F580-F599.
32. Regeer et al., 2004 R. R. Regeer and D. Markovich, A dileucine motif targets the sulfate anion transporter sat-1 to the basolateral membrane in renal cell lines. *Am J Physiol Cell Physiol.* **287**(2004), pp. C365-C372.
33. Romero et al., 2004 M. F. Romero, C. M. Fulton, and W. F. Boron, The SLC4 family of HCO 3 - transporters. *Pflugers Arch.* **447**(2004), pp. 495-509.
34. Romero, 2005 M.F. Romero, Molecular pathophysiology of SLC4 bicarbonate transporters. *Curr Opin Nephrol Hypertens.* **14**(2005): pp. 495-501.
35. Roussa et al., 1999 E. Roussa, M. F. Romero, B. M. Schmitt, W. F. Boron, S. L. Alper, and F. Thevenod, Immunolocalization of anion exchanger AE2 and Na(+)-HCO(-)(3) cotransporter in rat parotid and submandibular glands. *Am J Physiol* **277**(1999), G1288-G1296.
36. Scheiffele et al., 1995 P. Scheiffele, J. Peranen, and K. Simons, N-glycans as apical sorting signals in epithelial cells. *Nature* **378**(1995), pp. 96-98.
37. Schmitt et al., 1999 B. M. Schmitt, D. Biemesderfer, M. F. Romero, E. L. Bouppaep, and W. F. Boron, Immunolocalization of the electrogenic Na+-HCO-3 cotransporter in mammalian and amphibian kidney. *Am J Physiol Renal Physiol* **276**(1999), F27-F38.
38. Sheikh et al., 1996 H. Sheikh and C. M. Isacke, A di-hydrophobic Leu-Val motif regulates the basolateral localization of CD44 in polarized Madin-Darby canine kidney epithelial cells. *J. Biol.Chem.* **271**(1996), pp.12185-12190.
39. Simons et al., 1997 K. Simons and E. Ikonen, Functional rafts in cell membrane, *Nature*. **387**(1997), pp. 569-572.

40. Soleimani et al., 2001 M. Soleimani, and C. E. Burnham, Na+:HCO(3-) cotransporters (NBC): cloning and characterization. *J Membr Biol.* **183**(2001), pp. 71-84.
41. Soleimani, 2002 M. Soleimani, Na+:HCO3- cotransporters (NBC): expression and regulation in the kidney. *J Nephrol.* **15**(2002) Suppl 5, S32-40. Review.
42. Soleimani, 2003 M. Soleimani, Functional and molecular properties of Na+:HCO-3 cotransporters (NBC). *Minerva Urol Nefrol*. **55**(2003), pp.131-140
43. Tanemoto et al., 2005 M. Tanemoto, T. Abe, and S. Ito, PDZ-binding and di-hydrophobic motifs regulate distribution of Kir4.1 channels in renal cells. *J.Am.Soc.Nephrol.* **16**(2005), pp.2608-2614.
44. Tepass et al., 2001 U. Tepass, G. Tanentzapf, R. Ward, and R. Fehon, Epithelial cell polarity and cell junctions in *Drosophila. Annual Review of Genetics* **35**(2001), pp.747-784.
45. Theodore et al., 2003 R. M. Theodore and M. J. Caplan, Transport protein trafficking in polarized cells. *Annual Review of Cell and Developmental Biology*. **19**(2003), pp.333-366.
46. Thevenod et al., 1999 F. Thevenod, E. Roussa, B. M. Schmitt, and M. F. Romero, Cloning and immunolocalization of a rat pancreatic Na(+) bicarbonate cotransporter. *Biochem Biophys Res Commun* **264**(1999), pp. 291-298.
47. Thomas et al., 1993 D. C. Thomas, C. B. Brewer, and M. G. Roth, Vesicular stomatitis virus glycoprotein contains a dominant cytoplasmic basolatral sorting signal crtically dependent upon a tyrosin. *J. Biol.Chem.* **268**(1993), pp. 3313-3320.
48. Toye et al., 2006 A. M. Toye, M.D. Parker, C. M. Daly, J. Lu, L. V. Virkki, M. F. Pelletier and W. F. Boron. The Human NBCe1-A Mutant R881C, Associated With Proximal Renal Tubular Acidosis, Retains Function But Is Mistargeted In Polarized Renal Epithelia. *Am J Physiol Cell Physiol*. **291**(2006), C788-801.
49. Usui et al., 2001 T. Usui, M. Hara, H. Satoh, N. Moriyama, H. Kagaya, S. Amano, T. Oshika, Y. Ishii, N. Ibaraki, C. Hara, M. Kunimi, E. Noiri, K. Tsukamoto, J. Inatomi, H. Kawakami, H. Endou, T. Igarashi, A. Goto, T. Fujita, M. Araie, and G. Seki, G. Molecular basis of ocular abnormalities associated with proximal renal tubular acidosis. *J Clin Invest.* **108**(2001), pp. 107-115.
50. Xu et al., 2003 J. Xu, Z. H. Wang, S. Barone, M. Petrovic, H. Amlal, L. Conforti, S. Petrovic, and M. Soleimani, Expression of the Na+-HCO-3 cotransporter NBC4 in rat kidney and characterization of a novel NBC4 variant. *Am J Physiol Renal Physiol* **284**(2001), F41-50.
51. Yamada et al., 2003 H. Yamada, S. Yamazaki, N. Moriyama, C. Hara, S. Horita, Y. Enomoto, A. Kudo, H. Kawakami, Y. Tanaka, T. Fujita, G. and G. Seki, Localization of NBC-1 variants in human kidney and renal cell carcinoma. *Biochem Biophys Res Commun.* **310**(2003), pp. 1213-1218.
52. Zou et al., 2004 Z. Zou, B. Chung, T. Nguyen, S. Mentone, B. Thomson and D. Biemesderfer. Linking receptor-mediated endocytosis and cell signaling: evidence for regulated intramembrane proteolysis of megalin in proximal tubule. *J. Biol.Chem.* **279**(2004), pp.34302-10.

Fig. 1. Transfection of MDCK cells with GFP vector only (no NBC1 insert) or GFP-tagged wild type NBC1.

1a. Expression of GFP vector alone (no NBC1 insert).

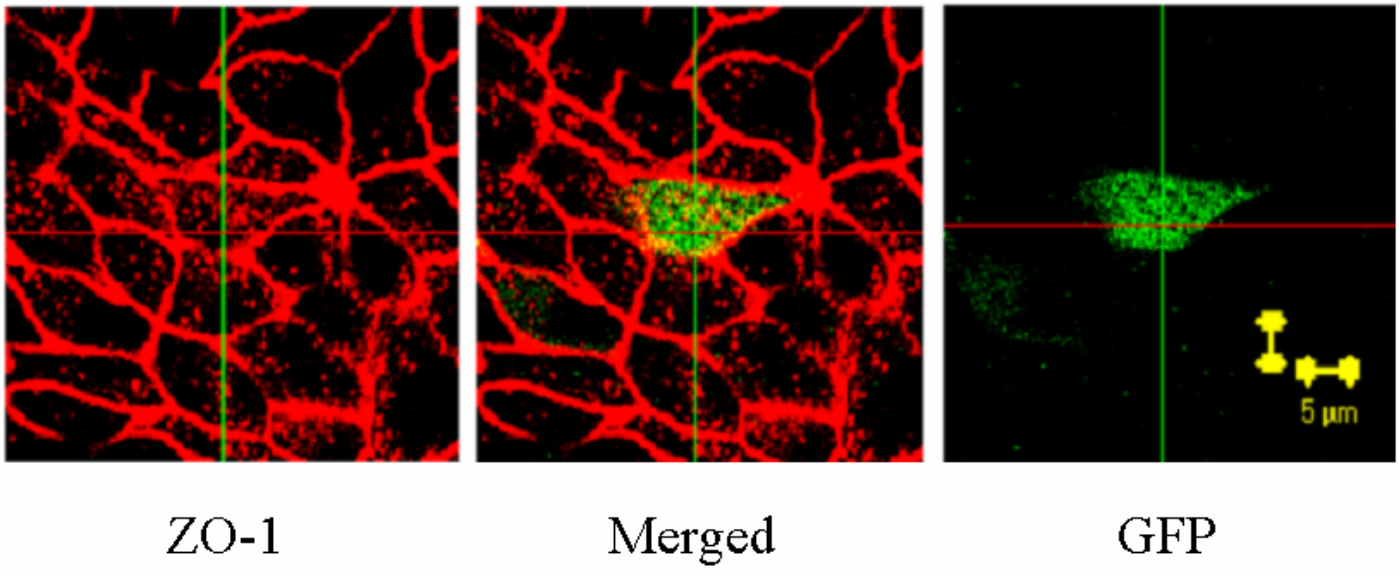

1b. Expression of epitope-tagged wild type NBC1 (1010 QQPFLS 1015)..

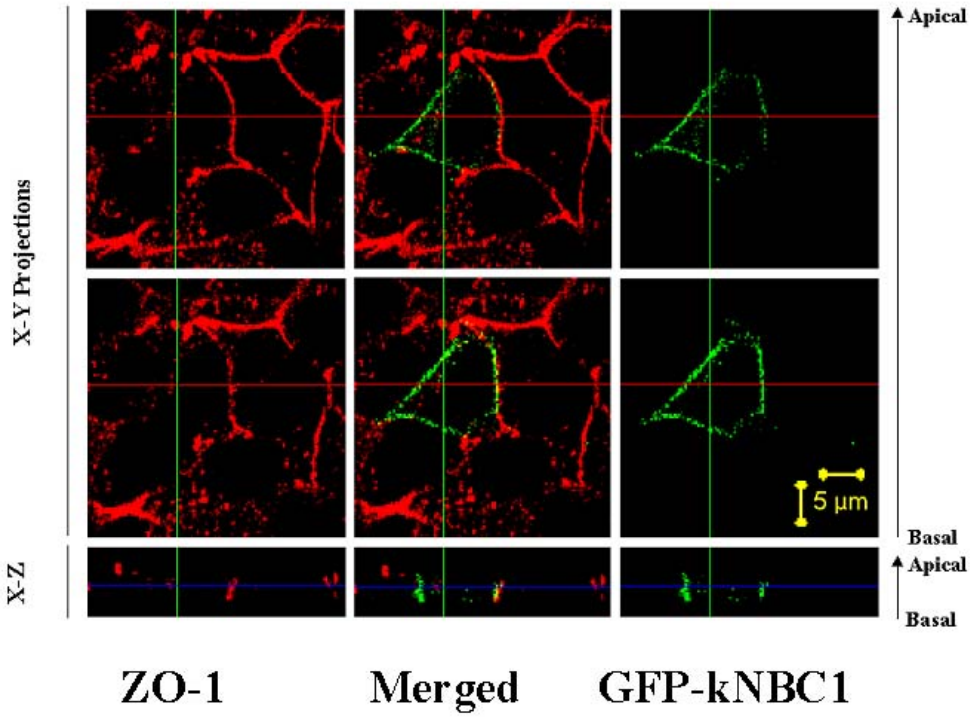

Fig. 2. Transfection of MDCK cells with the epitope tagged NBC1 mutants.

2a. Expression of the epitope-tagged NBC1 mutant 1 (1010 QQPLFS 1015)

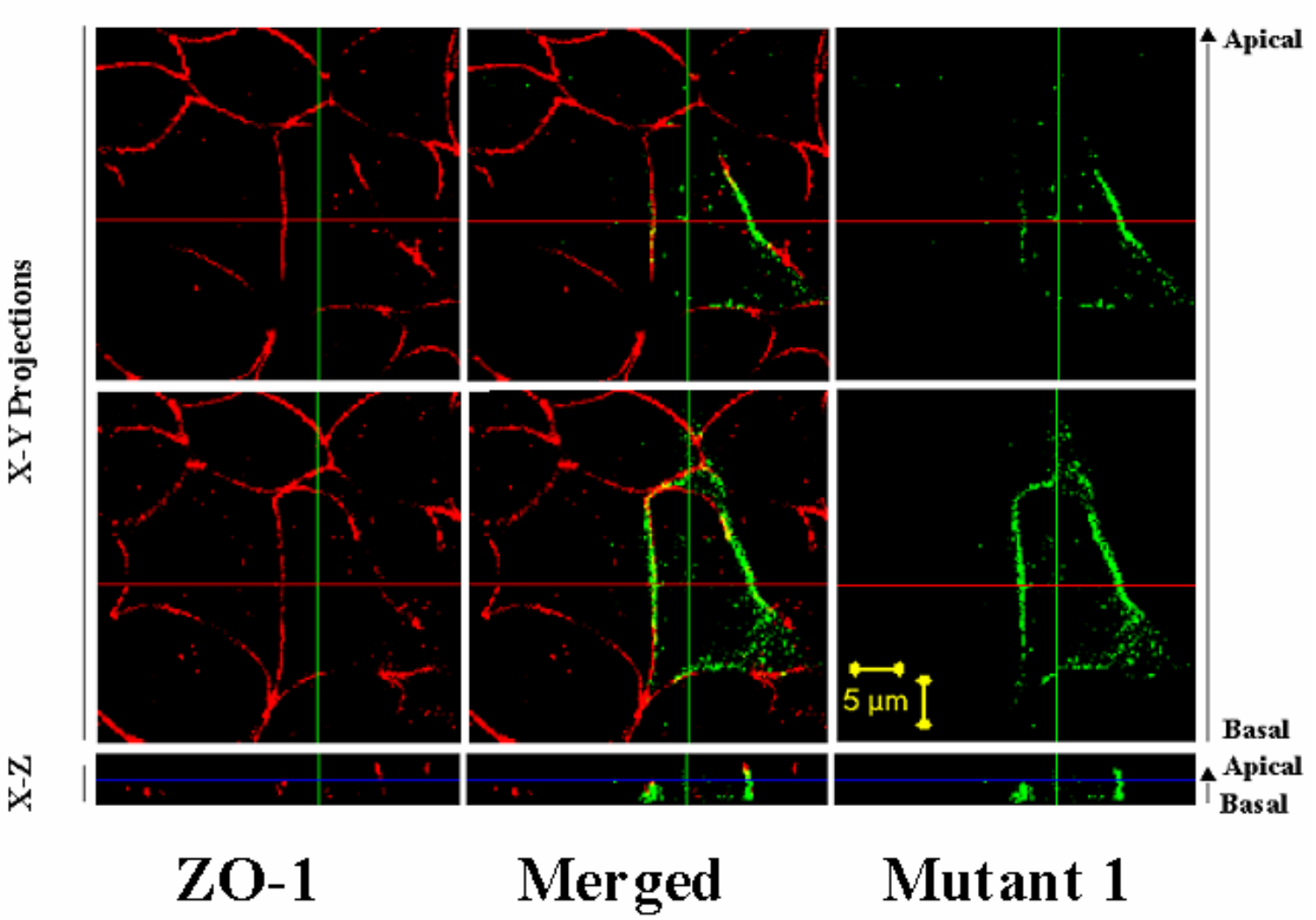

2b. Expression of the epitope-tagged NBC1 mutant 2 (1010 QQFLPS 1015).

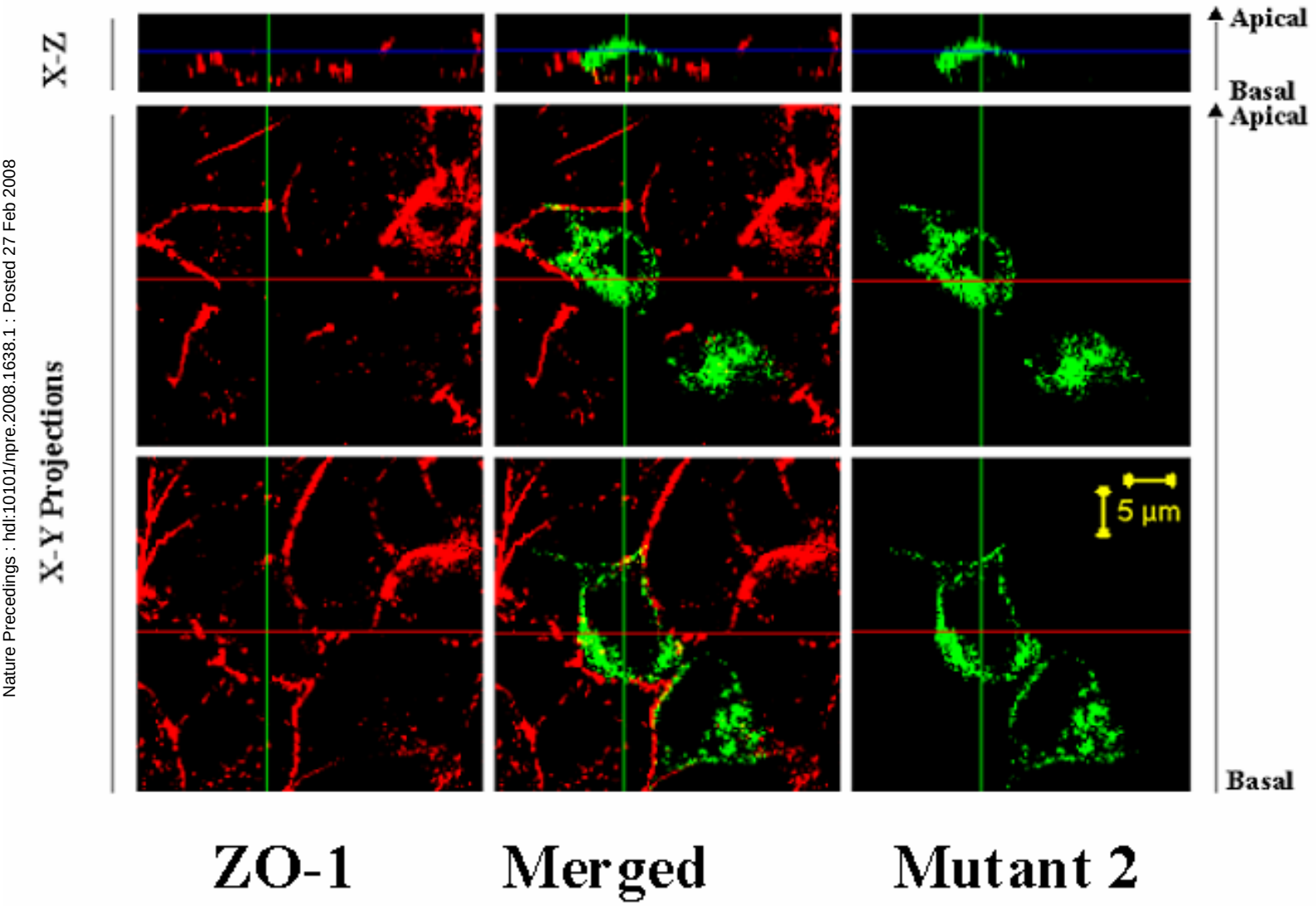

2c. Expression of the epitope-tagged NBC1 mutant 3 (1010 QQPSFL 1015).

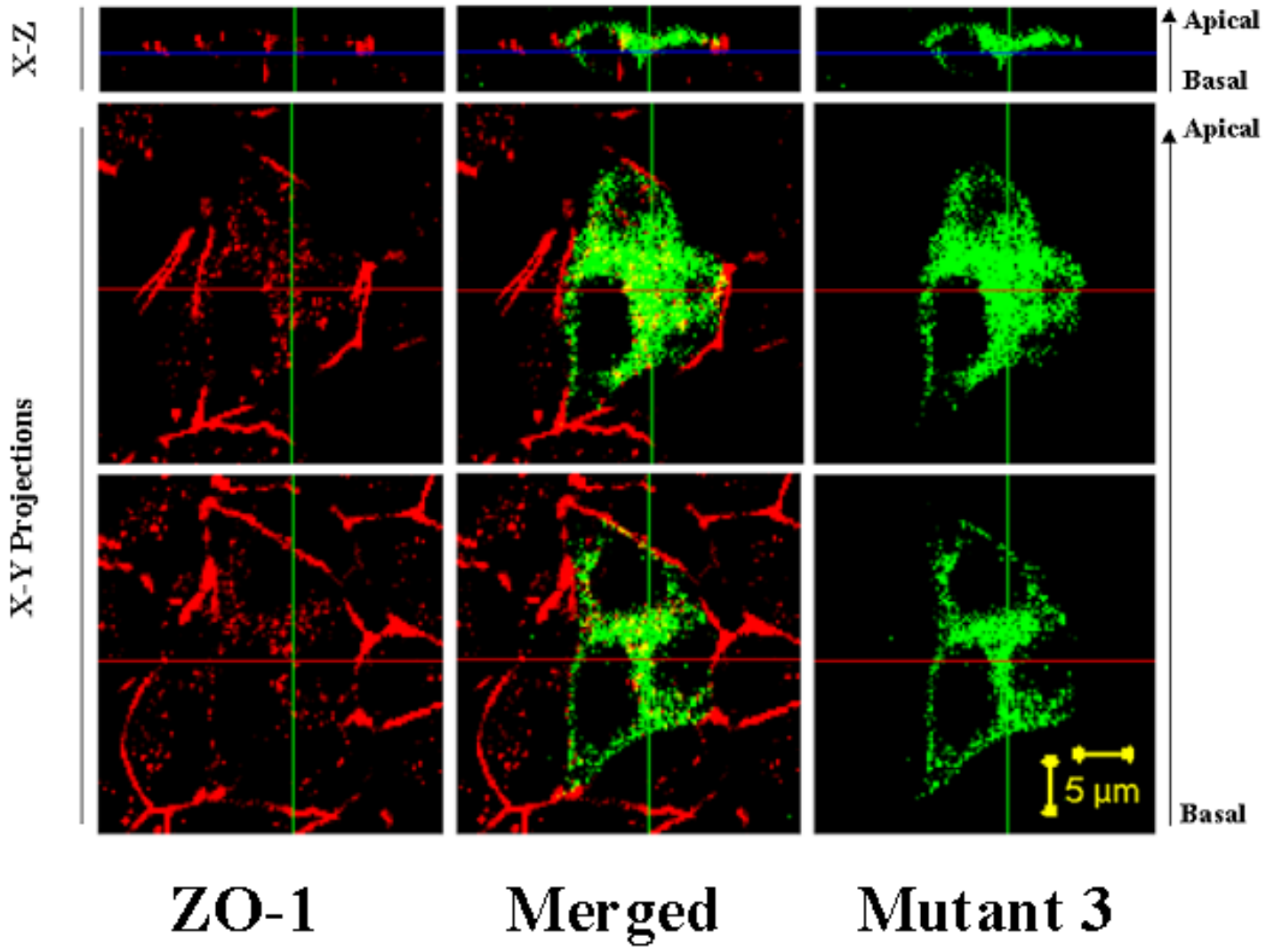

Fig. 3. Currents and voltage relationship of kNBC1 wild type and its mutants

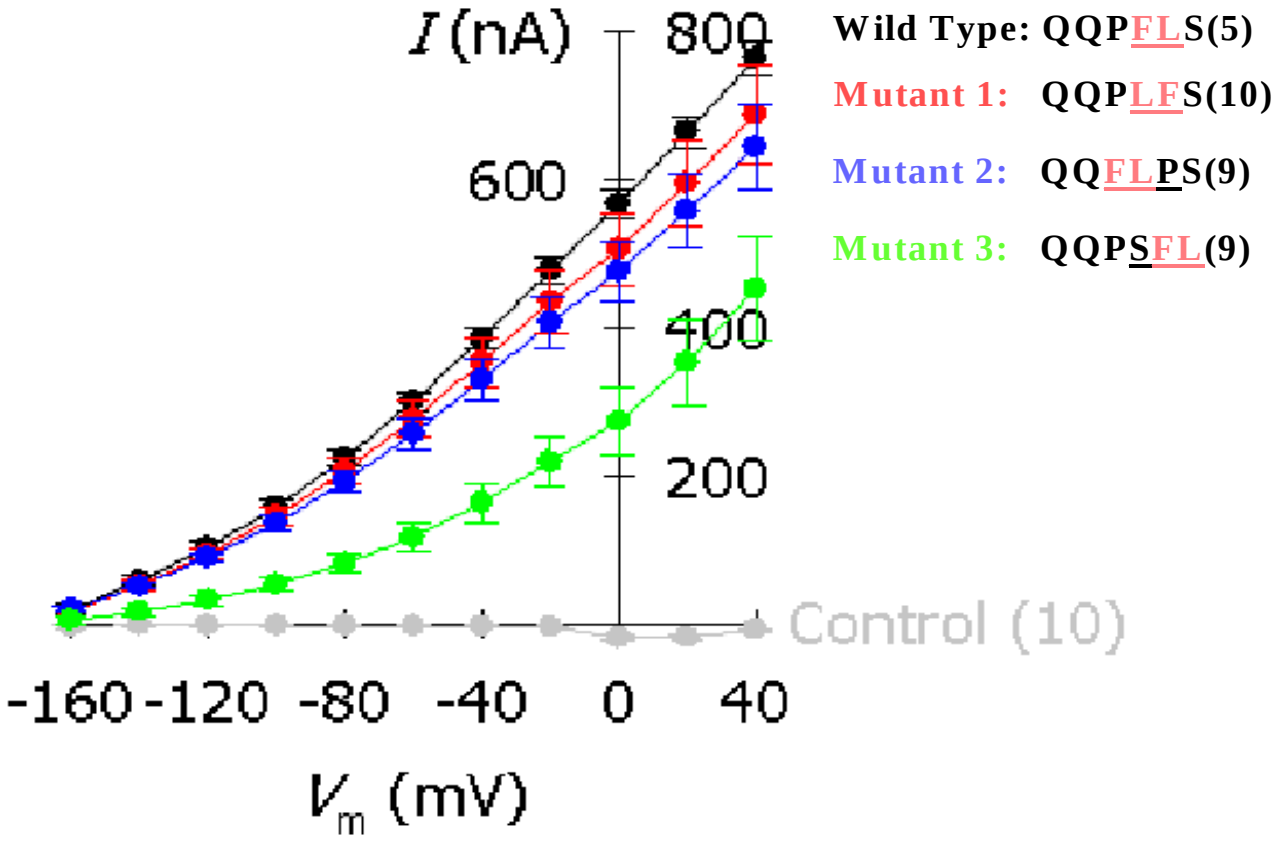

Fig. 4. Western blot analysis of the epitope-tagged kNBC1 and its mutants in frog oocytes.

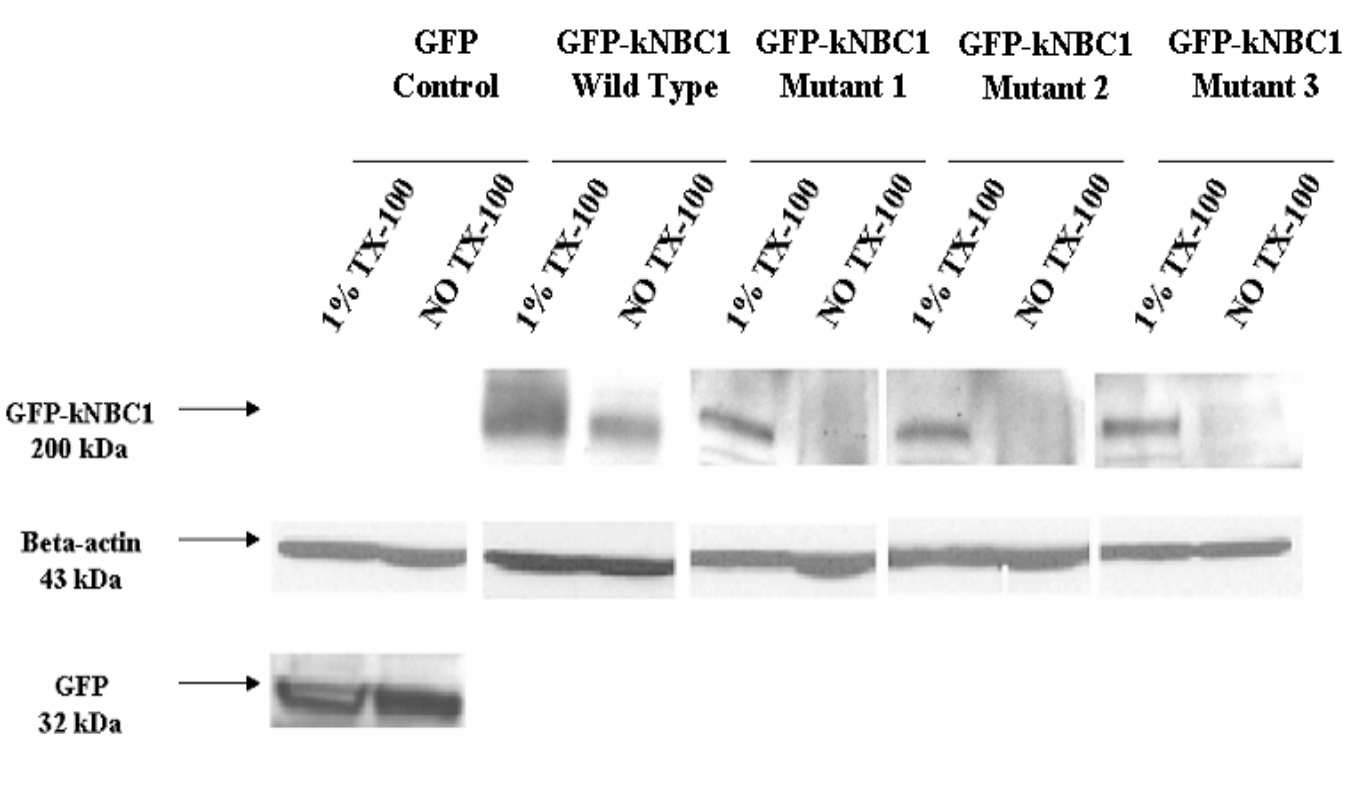

Fig. 5. Confocal images of sections of frog oocytes expressing epitope only, epitope-tagged kNBC1 wild type and mutant 3.

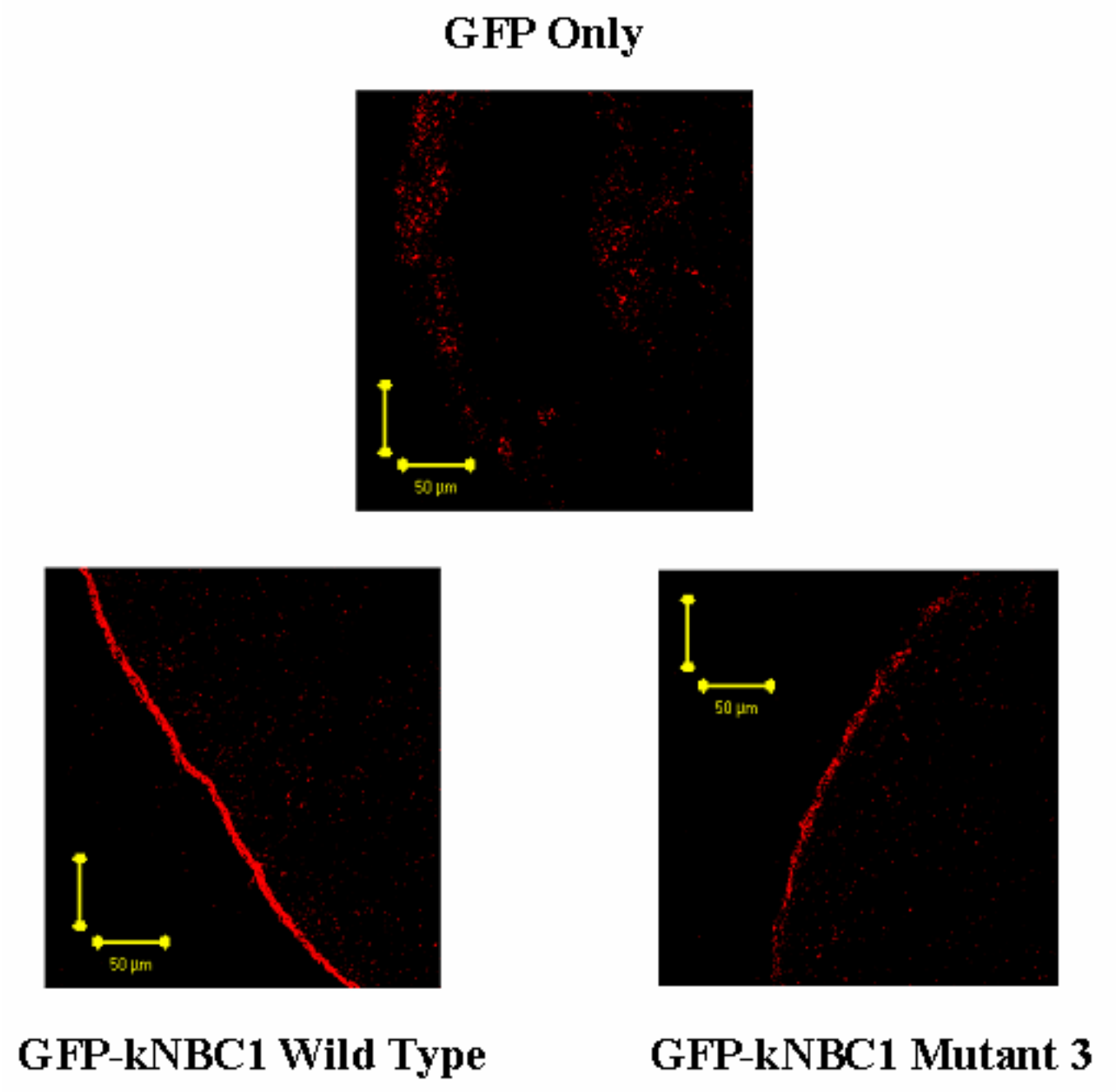

Fig.6. Immunostaining of MDCK cells expressing epitope-tagged kNBC1 wild type and mutant 3 with an ER marker antibody, PDI.

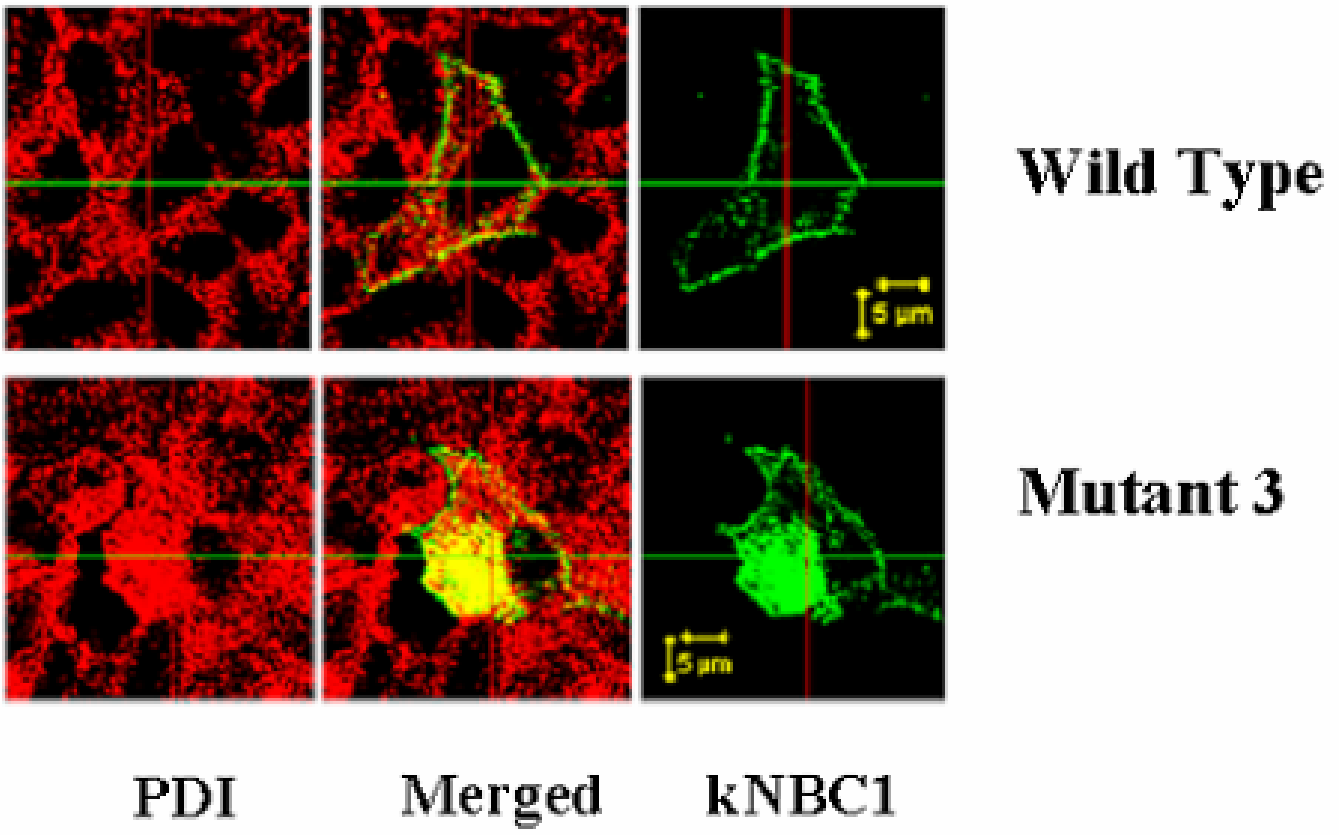

Fig.7. Circular dichroism comparison analysis of kNBC1 wild type and mutant short peptides

7a. CD spectra of kNBC1 wild type , mutant 1 and 3 short peptides in sodium phosphate buffer.

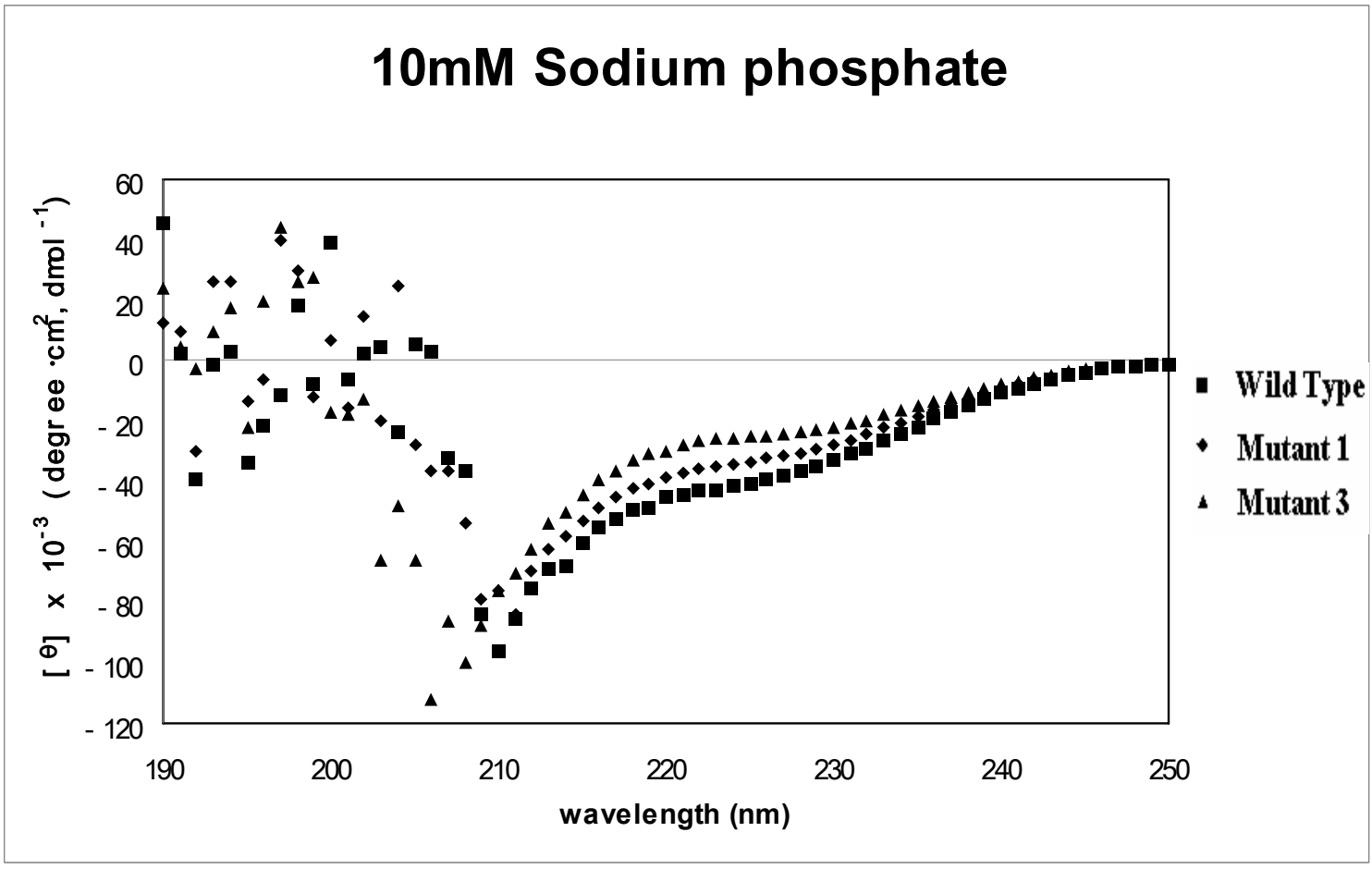

7b. CD spectra of kNBC1 wild type, mutant 1 and 3 short peptides in 50% TFE buffer.

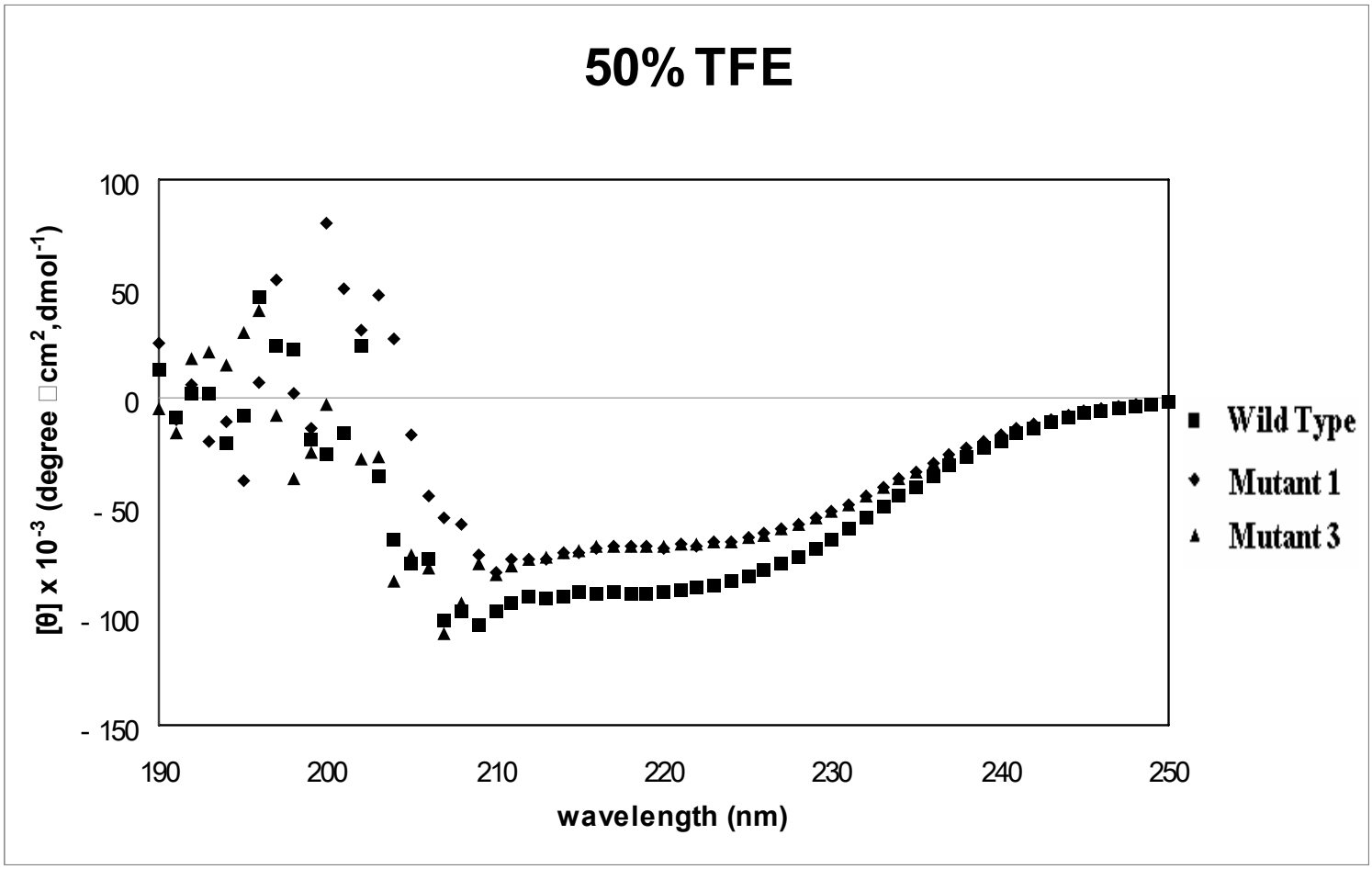

Table I. Analysis of CD spectra for secondary structure content of peptides

Peptide	Solvent	$[\theta]_{222}$[a]	% α-Helix[b]
Wild Type	SP[c]	-9406	27.3
	TFE	-18844	54.7
Mutant 1	SP[c]	-7791	22.6
	TFE	-14586	42.4
Mutant 3	SP[c]	-5800	16.8
	TFE	-14502	30.9

[a] Mean residue ellipticity is expressed in deg?cm^{2}?dmol^{-1}.
[b] Calculated by the equation under Materials and Methods.
[c] 10 mM sodium phosphate buffer.

Table II. A Summary of structures and functions of kNBC1 and mutants

kNBC1	Targeting	Alpha Helical Contents	Function
Wild Type PFLS	Basolateral	++++	*****
Mut1. W/ Reversal FL Motif PLFS	Basolateral	+++	*****
Mut2. W/ N-Terminal Shift FLPS	Apical & *cytoplasm*		*****
Mut3. W/ C-Terminal Shift PSFL	Cytoplasm & *Apical*	++	***